Supporting Information

Ultrasensitive Characterization of the Prion Protein by Surface-Enhanced Raman Scattering: Selective Enhancement via Electrostatic Tethering of the Intrinsically Disordered Domain with Functionalized Silver Nanoparticles

Swapnil Singh,[1,3†] Aishwarya Agarwal,[1,3†] Anamika Avni[1,2] and Samrat Mukhopadhyay[1,2,3] *

[1]Centre for Protein Science, Design and Engineering, [2]Department of Chemical Sciences, and [3]Department of Biological Sciences, Indian Institute of Science Education and Research (IISER), Mohali, Knowledge City, Mohali, Punjab, India

[†]These authors contributed equally.

*Corresponding author email: mukhopadhyay@iisermohali.ac.in

Materials

All the reagents used for the experiments were purchased from Sigma (St. Louis, MO) unless otherwise specified and were used as received. The glassware used for the experiments was washed with aqua regia and rinsed with Milli-Q water before use. Ultrapure Milli-Q water (18.2 MΩcm) was used for the preparation of buffers. The pH of the buffers was adjusted to the required final value (± 0.01) using a Metrohm 827 lab pH meter at room temperature (~ 25 ℃).

Methods

Preparation of silver nanoparticles

Silver nanoparticles (Ag NPs) were synthesized by the reduction of silver nitrate ($AgNO_3$) using the procedure described previously.[1,2] This method used for nanoparticle preparation produces a major population of quasi-spherical nanospheres along with a few nanorods. Briefly, 50 ml of 1 mM $AgNO_3$ solution was boiled (97 ±1 $^{\circ}$C) under vigorous stirring (1000 rpm) using a magnetic stirrer for 30 mins. After refluxing, 1.5 ml of 1% trisodium citrate was added to the reaction mixture and the reaction was allowed to proceed till the color turned yellow-green. The reaction mixture was then cooled at room temperature under stirring

conditions for another 30 mins and was further characterized using UV-vis absorption spectroscopy, scanning electron microscopy, and zeta potential measurements. Our nanoparticle preparation also yielded similar population distribution of quasi-spherical AgNPs (~ 40-60 nm) along with a few nanorods. We considered all of them for the size distribution and calculated the average size of the nanoparticles.

Preparation of halide modified nanoparticles

Halide modification of the Ag NPs was performed as described previously with slight modifications.[2] Briefly, Ag NPs were washed by centrifuging the 1 mL NPs colloidal suspension in a 1.5 ml microcentrifuge tube at 5000 rpm for 10 mins following which the supernatant was discarded and the precipitated colloid (~ 2-3 µL) was resuspended in 1 mL of Milli-Q water. The process was repeated, and the concentrated colloidal suspension (50 µL) was then mixed with 12 mM (50 µL) of potassium halide solutions and was incubated overnight at room temperature. In order to remove the excess halides, citrate, and other impurities present in the colloidal suspension, the halide modified NPs were centrifuged (5000 rpm, 10 min) and were resuspended in an equal amount of Milli-Q water (100 µL). The halide modified NPs (Ag IMNPs, Ag BrMNPs, Ag ClMNPs) were further characterized using absorption spectroscopy, SEM, and zeta potential measurements.

Protein expression and purification

The recombinant N-terminal His-tagged full-length human prion protein, PrP (23-231) cloned in pRSET B was expressed in *E.coli* strain BL21(DE3)pLysS and was purified as described previously.[3] The purified protein was then refolded using size-exclusion chromatography in 20 mM sodium phosphate buffer (pH 6.8). The stop mutant, PrP (Y145Stop) (23-144) was generated from the full-length human prion protein (23-231) by substituting the tyrosine codon at position 145 with a stop codon using site-directed mutagenesis.[4] The recombinant N-terminal His-tagged human prion protein (23-145) cloned in pRSET B was expressed in *E.coli* strain BL21(DE3)pLysS and was purified as described previously.[5] The purified protein was then refolded using size-exclusion chromatography in 20 mM sodium phosphate buffer (pH 7.3). The recombinant N-terminal His-tagged human prion protein (90-231) cloned in pQE-30 was expressed in SG13009(pREP4) and was purified as described previously.[3] The purified protein was then refolded using size-exclusion chromatography in 20 mM sodium phosphate buffer (pH; 7.3).

Absorption spectroscopy

All the absorption spectra were collected on a Thermo scientific multiskan GO UV-Vis spectrometer at room temperature (~ 25 °C). For these measurements, Ag NPs and halide modified NPs (Ag IMNPs, Ag BrMNPs, and Ag ClMNPs) were diluted 1000-fold whereas the solution of halide modified NPs with protein were diluted 100-fold.

Dynamic light scattering (DLS)

DLS measurements were carried out on a Malvern Zetasizer Nano ZS90 instrument (Malvern, UK) using a He–Ne laser (632 nm) as an excitation source. The zeta potential for Ag NPs and halide coated Ag NPs (I, Br, Cl) was an average of three scans and was recorded after diluting the sample 1000 times.

Scanning electron microscopy (SEM)

For SEM, 2.5 μL of 2000-fold diluted colloidal NPs were deposited on a silicon wafer and air-dried. The measurements were carried out using a field emission scanning electron microscope (FESEM), JSM-7600F (JEOL Inc., Japan) at an accelerating voltage of 15 kV.

Circular dichroism spectroscopy (CD)

For recording the far-UV CD spectra, protein concentrations of 10 μM were used with an average of three scans. The measurements were recorded on an Applied Photophysics Chirascan CD spectrometer at room temperature.

Atomic force microscopy (AFM)

AFM images of NPs and their aggregates were acquired on an Innova atomic force microscope (Bruker). The AFM was operated in the tapping mode. For imaging, the silicon nitride cantilever probe with a radius of ~8 nm was used. Before performing measurements, the samples were diluted 10-fold followed by which the 10 μL aliquots were withdrawn and deposited on freshly cleaved, water-washed muscovite mica (Grade V-4 mica from SPI, PA). The samples were allowed to incubate for 10 min at room temperature and were then washed with 200 μL of the ultrapure Milli-Q. Furthermore, the samples were kept under a gentle stream of nitrogen for 10 mins before scanning. The images were collected in NanoDrive

(v8.03) software at a resolution of 1024 × 1024 pixels. The collected AFM images were further processed and analyzed using WSxM version 5.0 Develop 9.1 software.[6]

Surface-enhanced Raman spectroscopy (SERS)

Bulk Raman and SERS spectra were recorded on an inVia dispersive laser Raman microscope with a 180° scattering geometry (Renishaw, UK) using a 785 nm laser excitation source which was focused on the sample using an objective lens (Nikon, Japan). The grating used was 1200 grooves/mm. Bulk Raman measurements of human PrP were done by drop deposition Raman spectroscopy (DDRS) method using a 300 mW laser power, 100x objective (NA = 0.9), 10 sec exposure time, and 25 accumulations. For SERS measurements, Ag IMNPs were mixed with aqueous protein solution in a 1:1 ratio (v/v) and a total volume of 50 µl was immediately added to an aluminum crucible. The final concentration of Ag IMNPs was fixed at ~2.5 nM, whereas final protein concentrations were 25 µM, 5 µM, 500 nM, and 250 nM. Also, SERS spectra for the respective buffers were recorded after Ag IMNPs addition [1:1 (v/v)] and were used for background subtraction. The beam was focused on the solution using a 3 mW laser power, a 20x objective (NA = 0.4), and a 10 sec exposure time. The measurements were repeated with different batches of protein and NPs with observed errors within the range of ±1 cm^{-1}. The Raman band of a silicon wafer at 520 cm^{-1} was used to calibrate the spectrometer and the spectral resolution was found to be ~ 0.5 cm^{-1}. The data were acquired using Wire 3.1 software provided with the spectrometer. All the data were corrected for tilt in the baseline using a cubic spline interpolation method in Wire 3.1 software. The baseline-corrected Raman spectra were finally plotted in Origin 8.5 software. The deconvolution of Raman spectra was done in Origin 8.5 software as described previously.[7]

The analytical enhancement factor (AEF) was estimated using the previously described method.[8] The peak at ~1445 cm^{-1} (C-H stretching) was used as the reference. Due to weak bulk solution Raman signals and the high protein concentration requirement, the AEF estimation was rather approximate using the following relationship:[8]

$$AEF = (I_{SERS}/C_{SERS})/(I_{Bulk}/C_{Bulk})$$

where, I_{SERS} and C_{SERS} correspond to the peak intensity and concentration of protein from the SERS signals, whereas, I_{Bulk} and C_{Bulk} refer to the peak intensity and concentration of the protein from Raman signals. For AEF estimation, the measurements were performed under identical experimental conditions (laser power, wavelength, microscope objective, etc.).

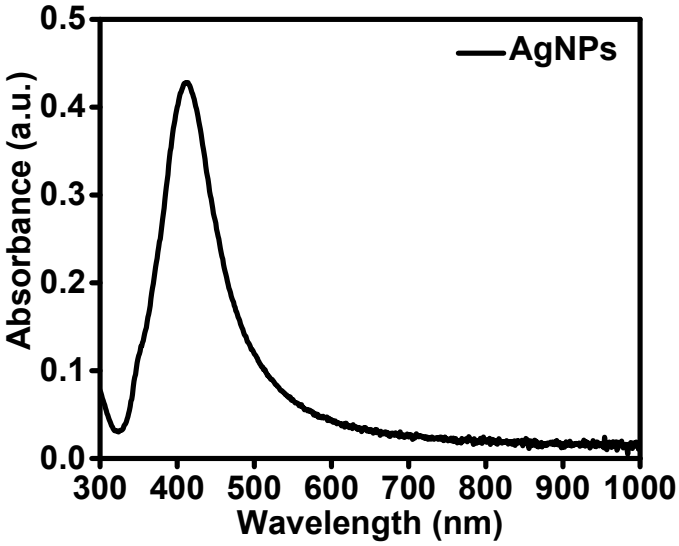

Figure S1. UV-Vis absorbance spectra for silver nanoparticles (Ag NPs)

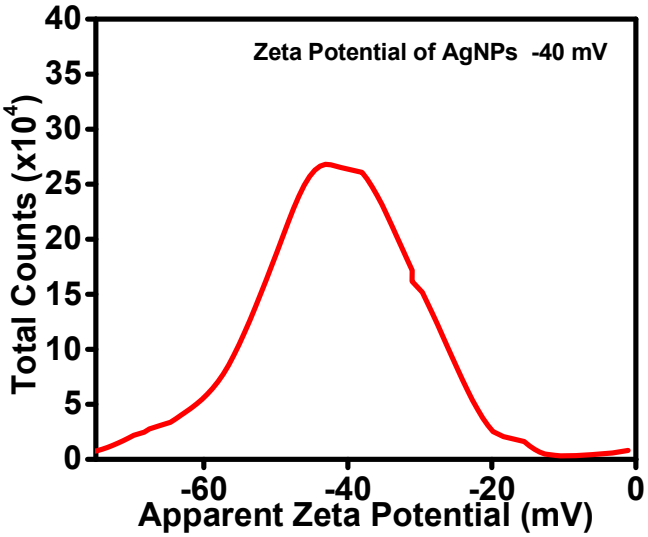

Figure S2. Zeta-potential for silver nanoparticles (Ag NPs)

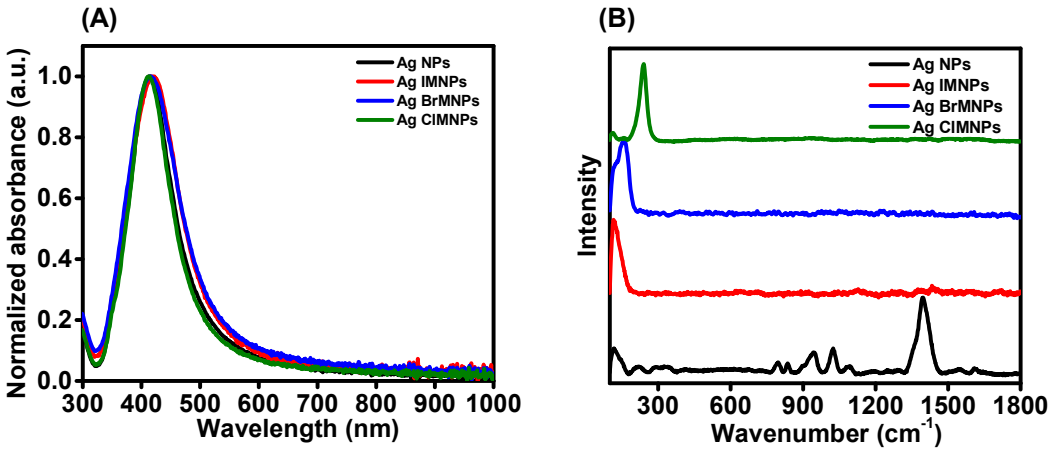

Figure S3. (A) UV-Vis absorbance spectra for silver colloids (Ag NPs) and halide (Cl, Br, I) functionalized Ag NPs. (B) SERS spectra for silver colloids (Ag NPs) and halide (Cl, Br, I) functionalized Ag NPs.

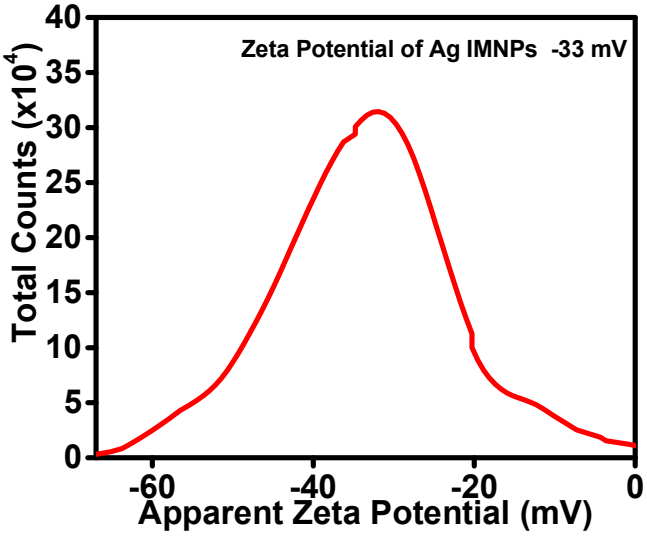

Figure S4. Zeta-potential for Ag IMNPs

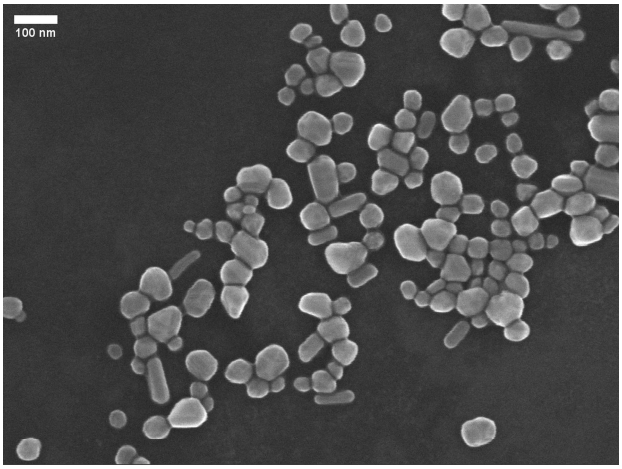

Figure S5. An SEM image of halide modified NPs (Ag IMNPs)

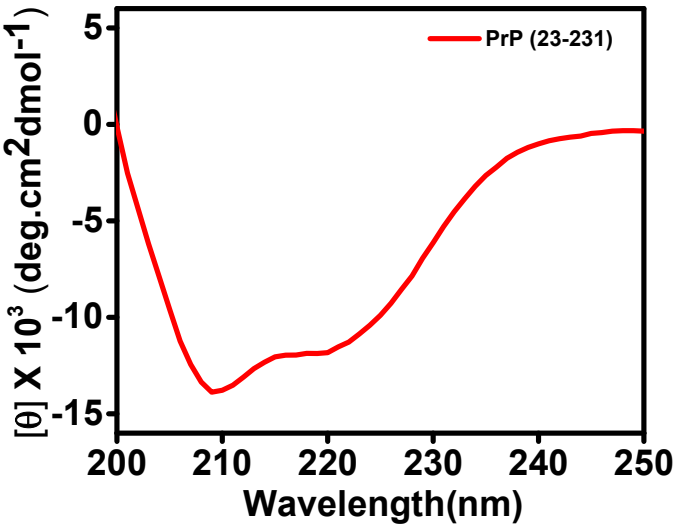

Figure S6. Far-UV CD spectra of PrP (23-231) in phosphate buffer (20 mM, pH 7.3)

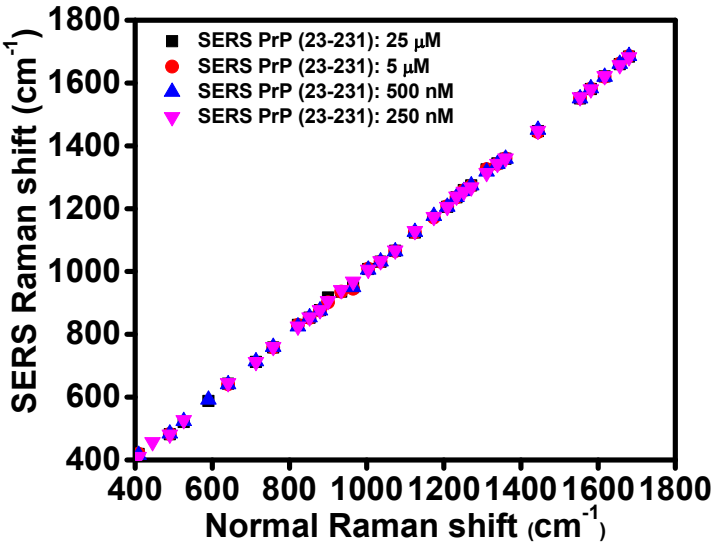

Figure S7. Correlation graph for PrP (23-231)

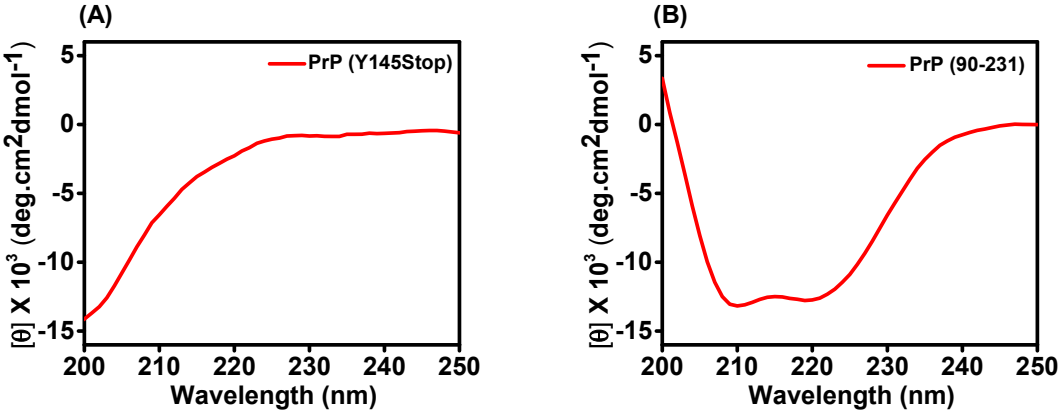

Figure S8. Far-UV CD spectra of (A) PrP (Y145Stop) (B) PrP (90-231) in phosphate buffer (20 mM, pH 7.3)

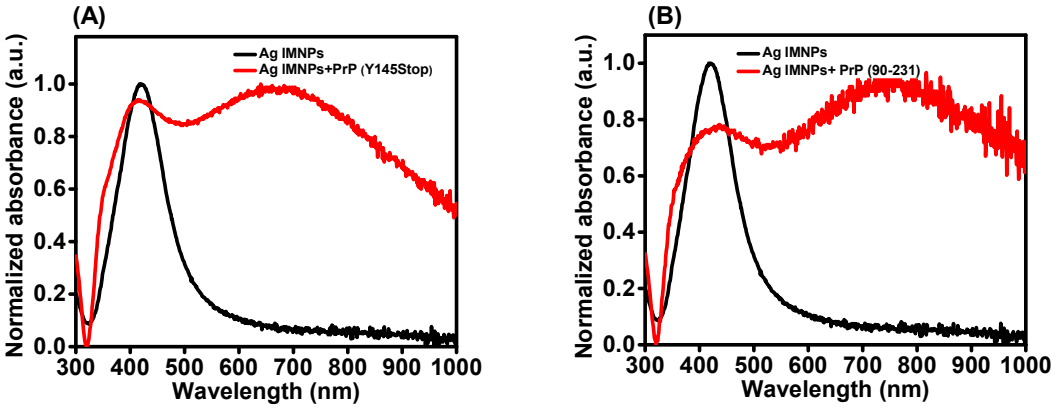

Figure S9. UV-Vis spectrum for Ag IMNPs: black and Ag IMNPs in presence of PrP: red (A) PrP (Y145Stop) (B) PrP (90-231)

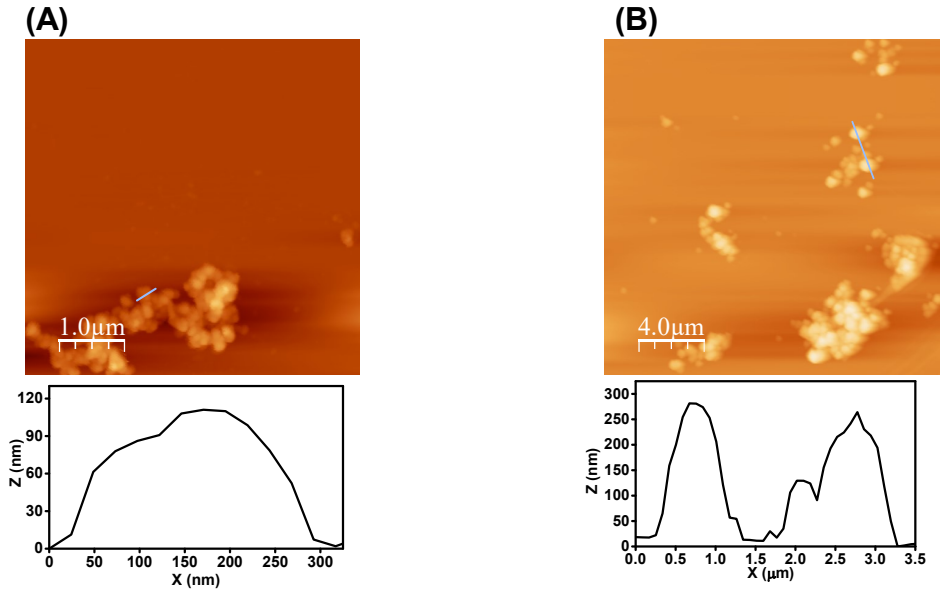

Figure S10. AFM image of Ag IMNPs aggregates in the presence of (A) PrP (Y145Stop) (B) PrP (90-231) with its respective height profile.

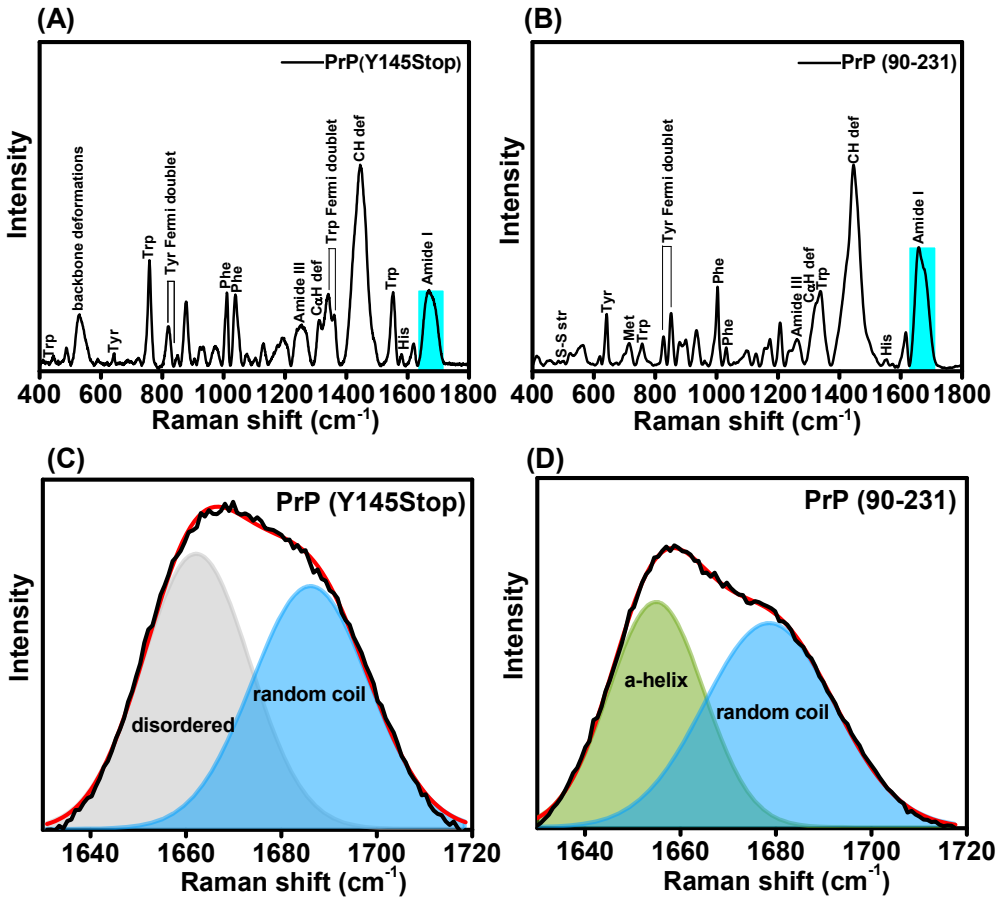

Figure S11. Bulk Raman spectra of (A) PrP (Y145Stop) and (B) PrP (90-231). The deconvolution of amide I (1630−1720 cm^{-1}) band for (C) PrP (Y145Stop) (D) PrP (90-231) The area under the curves represents the percentage contribution of secondary structure conformation (green: α-helix, grey: disordered, blue: random coil/extended conformation); The black spectrum is the raw data and red is the cumulative fit.

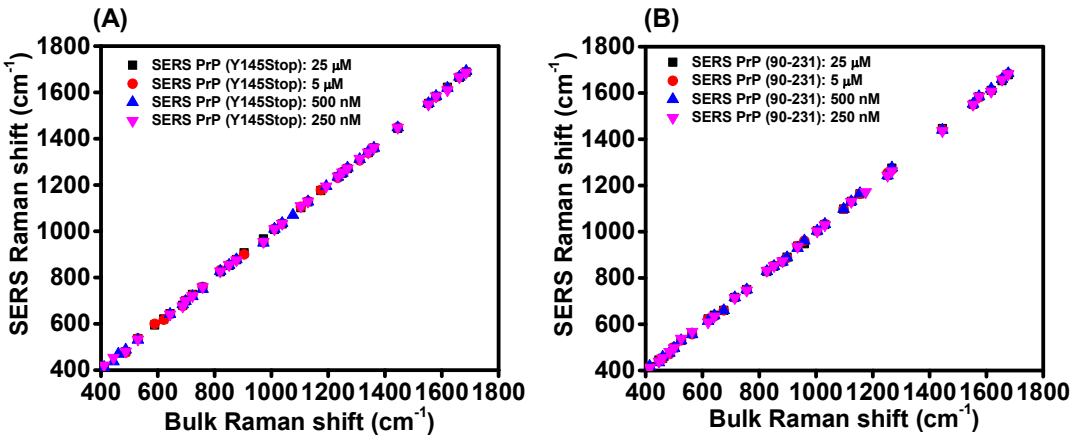

Figure S12. (A) Correlation graph for PrP (Y145Stop) (B) PrP (90-231).

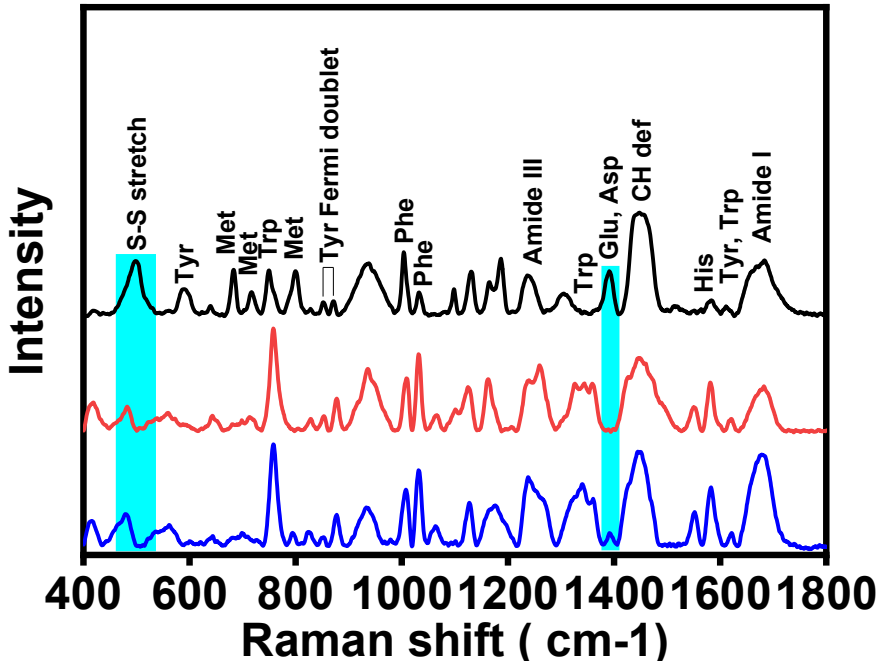

Figure S13. SERS spectra of different PrP constructs (25 µM). PrP (90-231): black, PrP (23-231): red, PrP (Y145Stop): blue.

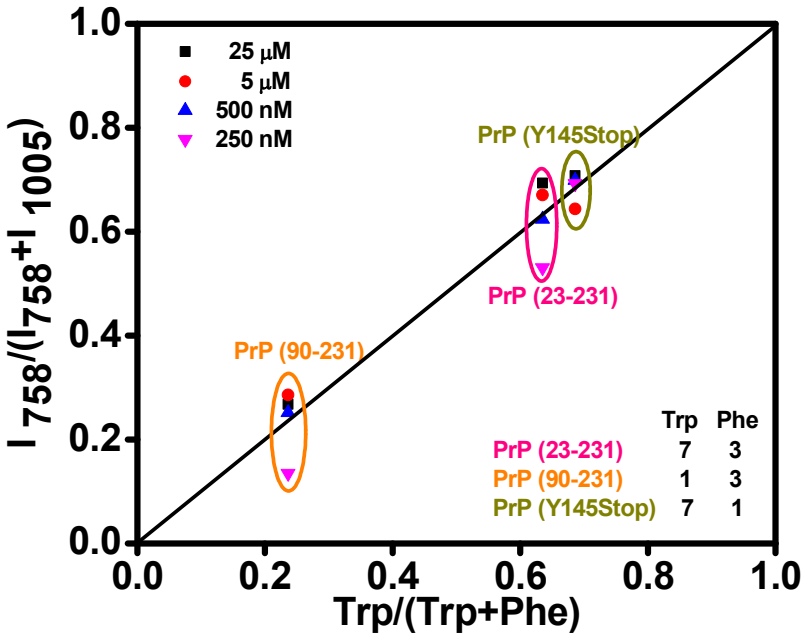

Figure S14. The plot between relative peak intensity ratios of Trp and Phe [$I_{758}/(I_{758}+I_{1005})$] against the ratio of [Trp/(Trp+Phe)] that represents the content of Trp and Phe from the SERS studies of three different constructs at different protein concentrations. The number of Trp and Phe residues are shown in the bottom right inset.

Table S1. Percentage contribution of different secondary structural elements obtained after deconvolution of the amide I (1630-1720 cm^{-1}) region from bulk Raman and SERS of prion protein constructs.

PrP constructs	α-helix (%)	Disordered (%)	Coils/Extended (%)
PrP 23-231 (Bulk)	27 ± 2.16	-	73 ± 2.16
PrP 23-231 (25 μM: SERS)	28 ± 7.79	-	72 ± 7.79
PrP 23-231 (250 nM: SERS)	30 ± 9.84	-	70 ± 9.84
PrP 90-231 (Bulk)	45 ± 1.25	-	55 ± 1.25
PrP 90-231 (25 μM: SERS)	44 ± 9.93	-	56 ± 9.93
PrP 90-231 (250 nM: SERS)	40 ± 10.80	-	60 ± 10.80
PrP Y145Stop (Bulk)	-	51 ± 2.16	49 ± 2.16
PrP Y145Stop (25 μM: SERS)	-	54 ± 2.94	46 ± 2.94
PrP Y145Stop (250 nM: SERS)	-	36 ± 9.20	64 ± 9.20

Table S2. Peak assignment of some selected modes of bulk Raman and SERS spectra of PrP (23-231), PrP (Y145Stop), and PrP (90-231).

	PrP 23-231 SERS 25 µM	**PrP 23-231 SERS 5 µM**	**PrP 23-231 SERS 500 nM**	**PrP 23-231 SERS 250 nM**	**PrP Y145Stop Bulk**	**PrP Y145Stop SERS 25 µM**	**PrP Y145Stop SERS 5 µM**	**PrP Y145Stop SERS 500 nM**	**PrP Y145Stop SERS 250 nM**	**PrP 90-231 Bulk**	**PrP 90-231 SERS 25 µM**	**PrP 90-231 SERS 5 µM**	**PrP 90-231 SERS 500 nM**	**PrP 90-231 SERS 250 nM**	**Peak Assignment[§,¶]**
1680	1683	1683	1685	1685	1686	1685	1687	1692	1685	1679	1681	1683	1688	1677	Am I (polyproline II/random β space)
1656	1658	1658	1658	1658	1662	1662	1666	1666	1663	1655	1655	1656	1659	1651	Am I (alpha/β sheet and disordered)
1617	1621	1620	1622	-	1620	1621	1618	1619	1610	1616	1611	1618	1611	-	Tyr, Trp
1580	1581	1582	1583	1580	1580	1583	1581	1584	1583	1586	1584	1585	1582	1585	His, Phe, Trp
1552	1551	1552	1551	1555	1553	1552	1553	1553	1548	1554	1551	-	1550	-	Trp
1445	1447	1444	1454	1448	1445	1445	1450	1448	1448	1446	1448	1440	1441	1438	$\delta[CH_2/CH_3]$
-	-	-	1396	-	-	1392	1389	-	-	-	1391	1391	1394	1390	Asp, Glu $\nu_s[COO^-]$
1358	1359	1361	1361	1360	1361	1360	1360	1360	1362	-	-	-	-	-	Trp
1340	1344	1342	1342	1344	1341	1340	1339	1344	1341	1339	1345	-	-	-	Trp/δ(CαH)
1273	1267	1269	1274	1275	1268	1271	1273	1272	1272	1267	1254	1255	1253	1261	Am III (alpha), ρ(CHα), Trp
1255	1257	1256	1256	1256	1250	1251	1256	1251	1255	1253	1240	1242	1241	1240	Am III

															(disordered/random)
1234	1236	1236	1236	1236	1234	1235	1236	1236	1236	1235	1230	1230	1231	1227	Am III (β sheet)
-	-	-	-	-	-	-	-	-	-	-	1186	1186	1187	1180	δ(C-H), Try, Phe
1174	1175	1173	1178	1174	1176	1176	1178	-	1179	1174	-	-	1173	1172	Tyr, Phe, ν[C-N]
-	1163	1163	1162	1163	1164	1167	-	1167	1162	-	1167	1166	1164	1166	Tyr, ν(Cβ-Cα-H), ν(C-C-H(R))
1120	1125	1125	1126	1129	1129	1127	1130	1129	1129	1128	1131	1131	1131	1129	ν[C-N], ν[C-C], Pro
1103	1101	1106	1107	-	1104	1101	1106	-	1109	1102	-	-	-	-	ν[C-C], ν[C-N], ν[C-O]
1053	1066	1065	1064	1067	-	1063	1062	-	1066	1066	1062	1065	1058	-	ν[C-C] of skeletal of random conformation ν[C-N], ν[C-O]
1036	1032	1032	1033	1034	1038	1032	1034	1035	1033	1032	1033	1034	1034	1032	Phe [δ(R(CH))]
1010	1009	1010	1007	1012	1011	1011	1011	1010	1010	-	-	-	-	-	Trp
1005	1005	1005	1004	1002	1005	1004	1005	-	1007	1003	1004	1004	1004	1001	Phe [$\delta(R_{breathing})$]
933	936	936	932	941	933	933	935	934	934	934	938	937	938	935	ν[N-C_α-C], Pro, Val
923	-	-	-	924	924	923	924	924	922	-	-	918	916	921	ν[N-C_α-C], Pro, Val
878	877	876	876	877	877	877	878	878	875	879	871	871	870	873	Trp [δ(R+r)]

852	854	853	855	855	851	853	855	854	854	852	852	853	854	853	Tyr [$\delta(R_{breathing})$]
822	829	827	825	825	820	825	832	828	826	827	828	829	829	832	Tyr [$\delta_{oop}(R_{breathing})$]
776	805	806	-	-	-	794	799	-	-	-	800	800	800	797	Met [ν_a(C-S-C)], Val, Tyr, δ[NH], ν[CH]
758	758	758	759	758	758	758	759	760	759	757	750	750	750	747	Trp [$\delta(R_{breathing})$]
710	712	-	714	712	722	727	724	-	720	715	716	716	715	714	Met [ν(C-S)]
682	682	-	684	-	688	680	-	684	-	687	683	683	682	683	Met [ν(C-S)], δCH]
641	643	641	641	645	643	644	642	642	-	642	639	638	642	633	Tyr [γ(C-C)]
526	521	-	524	527	530	536	537	531	533	524	530	-	531	-	δ[skeletal]
-	506	507	504	507	-	-	-	-	-	502	499	497	501	497	Cys [ν[(S-S)]
490	483	484	485	482	487	479	476	488	481	485	-	-	-	481	δ[Ring], τ[Ring]
410	419	421	417	421	411	414	424	413	411	413	417	419	417	412	Trp

§ δ, bending; τ, torsion; ν, stretching; γ, twisting; ρ, rocking; R, phenyl ring; r, pyrrole ring: a, asymmetric; s, symmetric

¶ The peak assignments have been described previously.[9-12]

References

1. Lee, P. C.; Meisel, D. Adsorption and Surface-Enhanced Raman of Dyes on Silver and Gold Sols. *J. Phys. Chem.* **1982**, 86, 3391–3395.
2. Xu, L. J.; Zong, C.; Zheng, X. S.; Hu, P.; Feng, J. M.; Ren, B. Label-Free Detection of Native Proteins by Surface-Enhanced Raman Spectroscopy Using Iodide-modified Nanoparticles. *Anal. Chem.* **2014**, 86, 2238–2245.
3. Agarwal, A.; Das, D.; Banerjee, T.; Mukhopadhyay, S. Energy Migration Captures Membrane-induced Oligomerization of the Prion Protein. *Biochim. Biophys. Acta - Proteins Proteomics* **2020***,* 1868, 140324(1-7).
4. Agarwal, A.; Rai. S. K.; Avni, A.; Mukhopadhyay, S. An Intrinsically Disordered Pathological Variant of the Prion Protein Y145Stop Transforms into Self-Templating Amyloids via Liquid-Liquid Phase Separation. *bioRxiv* 2021, http://doi.org/10.1101/2021.01.09.426049
5. Morillas, M.; Swietnicki, W.; Gambetti, P.; Surewicz, W. K. Membrane Environment Alters the Conformational Structure of the Recombinant Human Prion Protein Membrane Environment Alters the Conformational Structure of the Recombinant Human Prion Protein. *J. Biol. Chem.* **1999**, 274, 36859–36865.
6. Horcas, I.; Fernandez, R.; Gomez-Rodriguez, J. M.; Colchero, J.; Gomez-Herrero, J.; Baro, A. M. WSXM: A Software for Scanning Probe Microscopy and a Tool for Nanotechnology. *Rev. Sci. Instrum.* **2007**, 78, 13705(1-8).
7. Bhattacharya, M.; Jain, N.; Dogra, P.; Samai, S.; Mukhopadhyay, S. Nanoscopic Amyloid Pores Formed via Stepwise Protein Assembly. *J. Phys. Chem. Lett.* **2013**, 4, 480–485.
8. Le Ru, E. C.; Blackie, M.; Meyer, M.; Etchegoin, P. G. Surface-Enhanced Raman Scattering Enhancement Factors: A Comprehensive Study. *J. Phys. Chem. C.* **2007**, 111,13794-13803
9. Rygula, A.; Majzner, K.; Marzec, K. M.; Kaczor, A.; Pilarczyk, M.; Baranska, M. Raman Spectroscopy of Proteins: A review. *J. Raman Spectrosc.* **2013,** 44, 1061–1076.
10. Tuma, R. Raman Spectroscopy of Proteins: From Peptides to Large Assemblies. *J. Raman Spectrosc.* **2005**, 36, 307–319.
11. Szekeres, G. P.; Kneipp, J. SERS Probing of Proteins in Gold Nanoparticle Agglomerates. *Front. Chem.* **2019**, **7**, 30.
12. Mensch, C.; Bultinck, P.; Johannessen, C. Conformational Disorder and Dynamics of Proteins Sensed by Raman Optical Activity. *ACS Omega* **2018**, 3, 12944–12955.